SUPPLEMENTARY MATERIAL

Supplementary Figure S1. WRN activity on undamaged templates and on the templates incubated with HNE. (**A**) Effect of HNE treatment of 37 nt fork 22-15/22-15B oligodeoxynucleotide on WRN helicase activity. Radiolabeled template was preincubated with HNE and enzymatic assays were performed as described in Materials and Methods. (**B**) Percent of control helicase activity from the data shown in (**A**). (**C**) Effect of HNE treatment of 49 nt forked, TelX/TelY oligodeoxynucleotide on WRN exonuclease activity. Radiolabeled template was preincubated with HNE and enzymatic assays were performed. (**D**) Percent of control exonuclease activity from the data shown in (**C**). Mock, control enzymatic activity performed on templates that have been treated as HNE modified DNA but without HNE. Lane 5, heat denatured helicase substrate.

Supplementary Figure S2. Sequence of the WRN protein. MS peptide coverage is denoted in bold letters. Positions of the HNE adducted amino acids are indicated by big, red letters. Functional WRN domains are highlighted in light blue (exonuclease), green (helicase, including the Walker A motif, marked in yellow), magenta (RQC) and grey (HRDC). NLS is highlighted in dark blue.

Supplementary Figure S3. HNE modified WRN was characterized by LC-MS-MS/MS analysis. (**A**) Fragmentation spectrum of the ILPLMTIGM**H**LSQAVK peptide – modified at His1290. (**B**) Fragmentation spectrum of the HGPDSGLQPS**C**DVN**K** peptide – modified at Cys1367 and at Lys1371. (**C**) Fragmentation spectrum of the S**K**EEVGINTETSSAER peptide – modified at Lys1389. During fragmentation, peptide dissociates into two fragments. Fragments containing the N terminal part of the peptides are termed b series ions (singly "b" and doubly "b++" charged), and, respectively, fragments containing the C terminal part are named y series ions (singly "y" and doubly "y++" charged) (51). Tables represent a list of theoretical fragment ions calculated by the Mascot program, which served to identify modified peptide (fragment ions found in the spectra are shadowed). Assignment of dominating peaks from the spectra to the theoretical fragmentation ions definitely confirms the modification.

Supplementary Figure S4. Modeled structure of helicase and RQC domain of the WRN protein. (**A**) Stereo view of the hybrid model of the WRN protein helicase and RQC domain (521–1089 aa). The model was derived as a combination of 20 homology models built independently on the basis of *E. coli* RecQ catalytic core (PDB IDs: 1OYW and 1OYY) and human RECQL1 (PDB IDs: 2WWY and 2V1X). ADP molecule bound structure built on the basis of human RECQL1 is represented by magenta balls. Magnesium ion is marked as yellow ball. (**B**) Ribbon representations of WRN modeled structure (dark blue) and structures of *E. coli* RecQ (1OYW – orange, 1OYY – cyan) and human RECQL1 (2WWY – grey, 2V1X – magenta) are superimposed. (**C**) Stereo view of helicase and RQC domain of the WRN protein with HNE modifications. Side chains of Lys577 and Cys727, which undergo HNE addition, are denoted as red balls. The ADP residue is shown as magenta balls. Magnesium ion is marked as a yellow ball. (**D**) The helicase and RQC domain of the WRN protein with HNE adducted Lys577 and Cys727 and bound DNA substrate. DNA molecule built on the basis of human RECQL1 (2WWY) is represented by grey sticks.

Supplementary Figure S5. Stereo view of structural changes in helicase and RQC domains of WRN protein upon HNE adduction. The molecular surface representation of helicase and RQC domains of the WRN protein with electrostatic potential (±25 kT/e, red-negative, blue-positive, grey-neutral) before (**A**) and after HNE addition to Lys577 (**B**). A comparison of the vicinity of native (**C**) and adducted Lys577 (**D**) shows some changes in molecular surface around the ATP (ADP) binding pocket. (**E**) Surface representation of helicase and RQC domains of the WRN protein after orthogonal rotation along the Y axis of 45° in relation to the structure shown in (**A**). (**F**) Surface representation of helicase and RQC domains of the WRN protein with HNE adducted at Cys727. A closer view of unadducted (**G**) and adducted Lys727 (**H**) illustrates changes in atom charge and points to surface location of HNE adducted to Lys727.

Figure S1

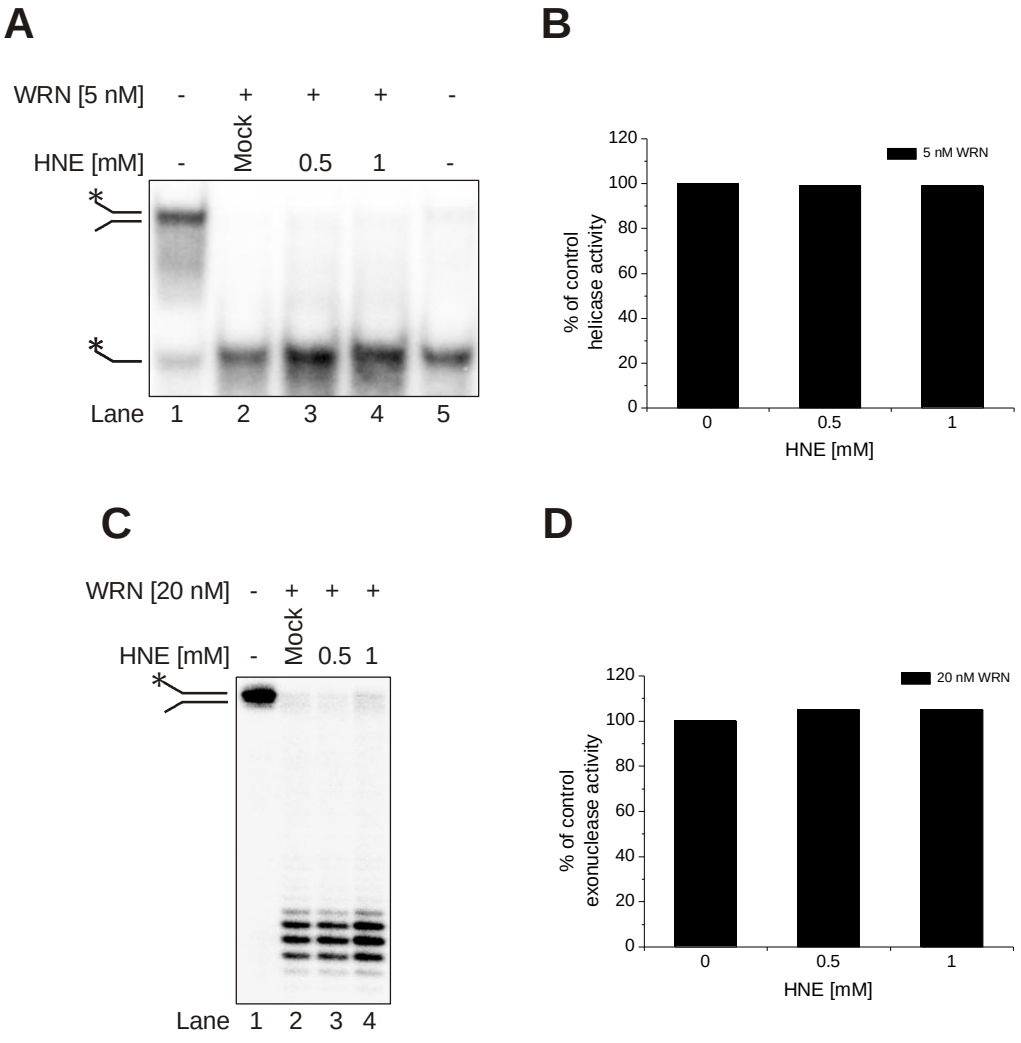
A
WRN [5 nM] - + + + -
HNE [mM] - Mock 0.5 1 -
Lane 1 2 3 4 5
B
5 nM WRN
% of control helicase activity
120
100
80
60
40
20
0
0 0.5 1
HNE [mM]
C
WRN [20 nM] - + + +
HNE [mM] - Mock 0.5 1
Lane 1 2 3 4
D
20 nM WRN
% of control exonuclease activity
120
100
80
60
40
20
0
0 0.5 1
HNE [mM]

Figure S2

1 MSEKKLETTA QQRKCPEWMN VQNKRCAVEE RKACVRKSVF EDDLPFLEFT
51 GSIVYSYDAS DCSFLSEDIS MSLSDGDVVG FDMEWPPLYN RGKLGKVALI
101 QLCVSESKCY LFHVSSMSVF PQGLKMLLEN KAVKKAGVGI EGDQWKLLRD
151 FDIKLKNFVE LTDVANKKLK CTETWSLNSL VKHLLGKQLL KDKSIRCSNW
201 SKFPLTEDQK LYAATDAYAG FIIYRNLEIL DDTVQRFAIN KEEEILLSDM
251 NKQLTSISEE VMDLAKHLPH AFSKLENPRR VSILLKDISE NLYSLRRMII
301 GSTNIETELR PSNNLNLLSF EDSTTGGVQQ KQIREHEVLI HVEDETWDPT
351 LDHLAKHDGE DVLGNKVERK EDGFEDGVED NKLKENMERA CLMSLDITEH
401 ELQILEQQSQ EEYLSDIAYK STEHLSPNDN ENDTSYVIES DEDLEMEMLK
451 HLSPNDNEND TSYVIESDED LEMEMLKSLE NLNSGTVEPT HSKCLKMERN
501 LGLPTKEEEE DDENEANEGE EDDDKDFLWP APNEEQVTCL KMYFGHSSFK
551 PVQWKVIHSV LEERRDNVAV MATGYGKSLC FQYPPVYVGK IGLVISPLIS
601 LMEDQVLQLK MSNIPACFLG SAQSENVLTD IKLGKYRIVY VTPEYCSGNM
651 GLLQQLEADI GITLIAVDEA HCISEWGHDF RDSFRKLGSL KTALPMVPIV
701 ALTATASSSI REDIVRCLNL RNPQITCTGF DRPNLYLEVR RKTGNILQDL
751 QPFLVKTSSH WEFEGPTIIY CPSRKMTQQV TGELRKLNLS CGTYHAGMSF
801 STRKDIHHRF VRDEIQCVIA TIAFGMGINK ADIRQVIHYG APKDMESYYQ
851 EIGRAGRDGL QSSCHVLWAP ADINLNRHLL TEIRNEKFRL YKLKMMAKME
901 KYLHSSRCRR QIILSHFEDK QVQKASLGIM GTEKCCDNCR SRLDHCYSMD
951 DSEDTSWDFG PQAFKLLSAV DILGEKFGIG LPILFLRGSN SQRLADQYRR
1001 HSLFGTGKDQ TESWWKAFSR QLITEGFLVE VSRYNKFMKI CALTKKGRNW
1051 LHKANTESQS LILQANEELC PKKLLLPSSK TVSSGTKEHC YNQVPVELST
1101 EKKSNLEKLY SYKPCDKISS GSNISKKSIM VQSPEKAYSS SQPVISAQEQ
1151 ETQIVLYGKL VEARQKHANK MDVPPAILAT NKILVDMAKM RPTTVENVKR
1201 IDGVSEGKAA MLAPLLEVIK HFCQTNSVQT DLFSSTKPQE EQKTSLVAKN
1251 KICTLSQSMA ITYSLFQEKK MPLKSIAESR ILPLMTIGMH LSQAVKAGCP
1301 LDLERAGLTP EVQKIIADVI RNPPVNSDMS KISLIRMLVP ENIDTYLIHM
1351 AIEILKHGPD SGLQPSCDVN KRRCFPGSEE ICSSSKRSKE EVGINTETSS
1401 AERKRRLPVW FAKGSDTSKK LMDKTKRGGL FS

Figure S3

A

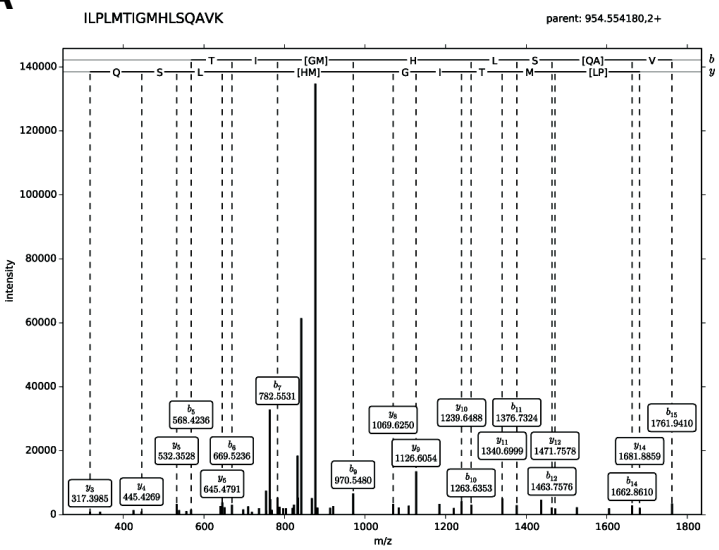

ILPLMTIGM**H**LSQAVK

#	b	b^{++}	Seq.	y	y^{++}	#
1	114.09	57.54	**I**			**16**
2	227.17	114.09	**L**	1795.02	898.01	**15**
3	324.22	162.61	**P**	**1681.93**	**841.47**	**14**
4	437.31	219.15	**L**	1584.88	792.94	**13**
5	**568.35**	284.68	**M**	**1471.80**	736.40	**12**
6	**669.40**	335.20	**T**	**1340.76**	670.88	**11**
7	**782.48**	391.74	**I**	**1239.71**	620.36	**10**
8	839.50	420.25	**G**	**1126.62**	563.81	**9**
9	**970.54**	485.77	**M**	**1069.60**	535.30	**8**
10	**1263.72**	632.36	**H**	938.56	469.78	**7**
11	**1376.80**	688.90	**L**	**645.39**	323.20	**6**
12	**1463.83**	732.42	**S**	**532.30**	266.65	**5**
13	1591.89	796.45	**Q**	**445.27**	223.14	**4**
14	**1662.93**	**831.96**	**A**	**317.21**	159.11	**3**
15	**1762.00**	881.50	**V**	246.18	123.59	**2**
16			**K**	147.11	74.06	**1**

B

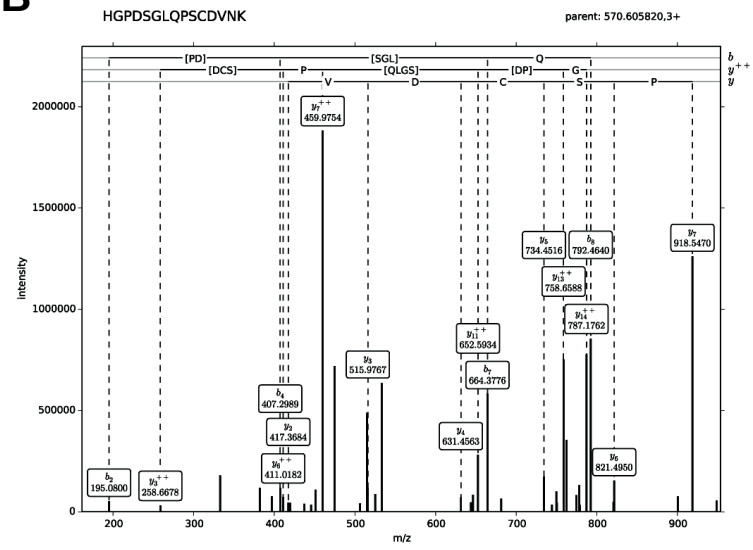

HGPDSGLQPS**C**DVN**K**

#	b	b^{++}	Seq.	y	y^{++}	#
1	138.06	69.53	**H**			**15**
2	**195.08**	98.04	**G**	1572.75	**786.88**	**14**
3	292.14	146.57	**P**	1515.73	**758.37**	**13**
4	**407.16**	204.08	**D**	1418.68	709.84	**12**
5	494.19	247.60	**S**	1303.65	**652.33**	**11**
6	551.22	276.11	**G**	1216.62	608.81	**10**
7	**664.30**	**332.65**	**L**	1159.60	580.30	**9**
8	**792.36**	**396.68**	**Q**	1046.51	523.76	**8**
9	889.41	445.21	**P**	**918.46**	**459.73**	**7**
10	976.44	488.72	**S**	**821.40**	**411.20**	**6**
11	1079.45	540.23	**C**	**734.37**	367.69	**5**
12	1194.48	597.74	**D**	**631.36**	316.18	**4**
13	1293.55	647.28	**V**	**516.33**	**258.67**	**3**
14	1407.59	704.30	**N**	**417.27**	209.13	**2**
15			**K**	303.22	152.11	**1**

Figure S3

C

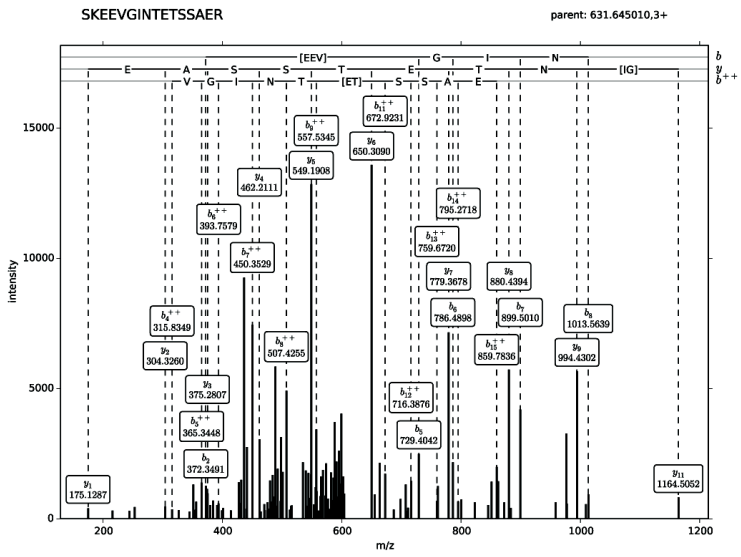

SKEEVGINTETSSAER

#	b	b^{++}	Seq.	y	y^{++}	#
1	88.0	44.52	**S**			**16**
2	**372.24**	186.62	**K**	1805.91	903.46	**15**
3	501.29	251.14	**E**	1521.70	**761.35**	**14**
4	630.33	**315.67**	**E**	1392.66	696.83	**13**
5	**729.40**	**365.20**	**V**	1263.61	632.31	**12**
6	**786.42**	**393.71**	**G**	**1164.54**	**582.77**	**11**
7	**899.50**	**450.25**	**I**	1107.52	554.26	**10**
8	**1013.55**	**507.27**	**N**	**994.44**	497.72	**9**
9	1114.59	**557.80**	**T**	**880.40**	440.70	**8**
10	1243.64	622.32	**E**	**779.35**	390.18	**7**
11	1344.68	**672.84**	**T**	**650.31**	325.65	**6**
12	1431.72	**716.36**	**S**	**549.26**	275.13	**5**
13	1518.75	**759.88**	**S**	**462.23**	231.61	**4**
14	1589.79	**795.39**	**A**	**375.19**	188.10	**3**
15	1718.83	**859.92**	**E**	**304.16**	152.58	**2**
16			**R**	**175.11**	88.06	**1**

Figure S4

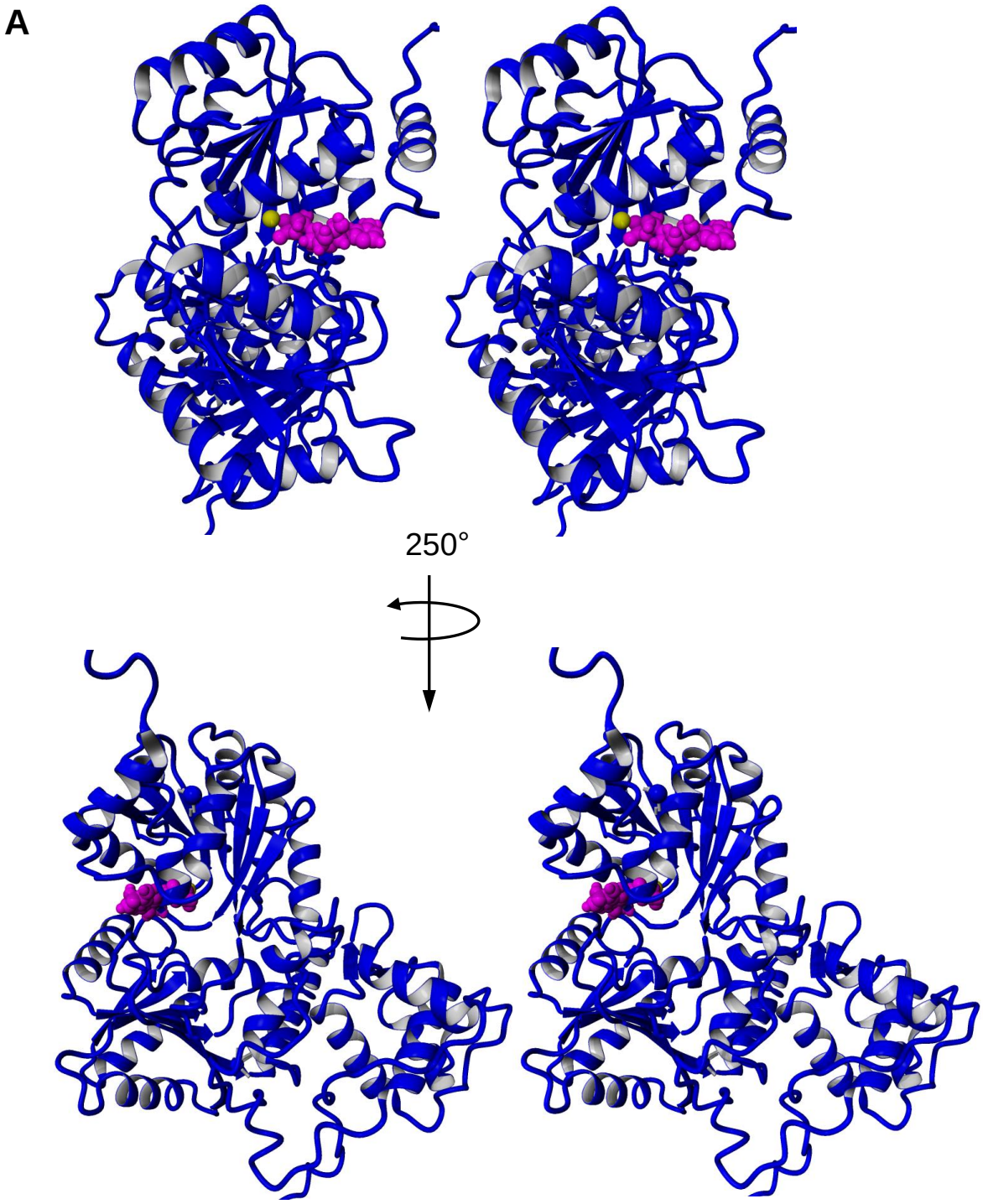

Figure S4

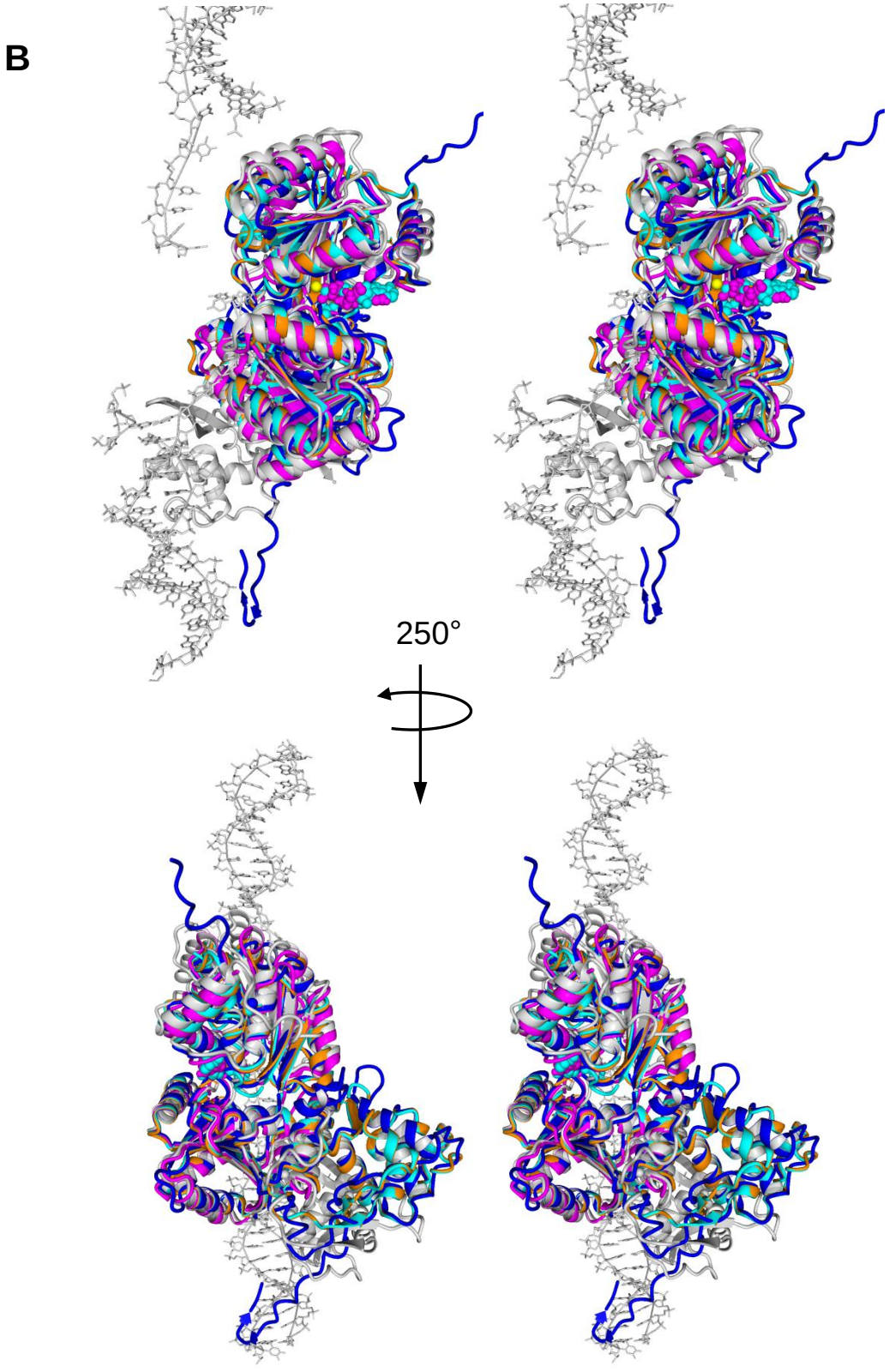

Figure S4

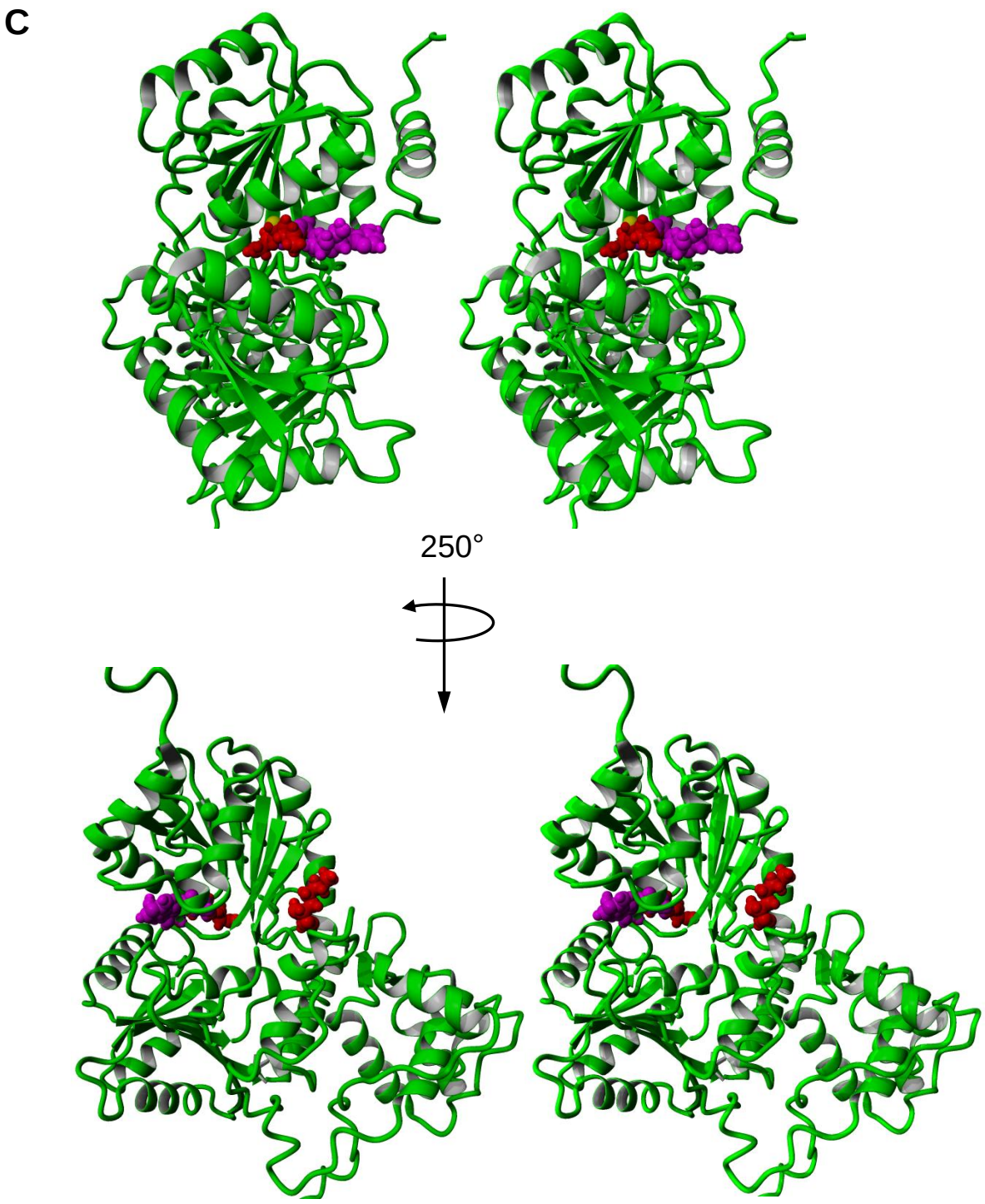

Figure S4

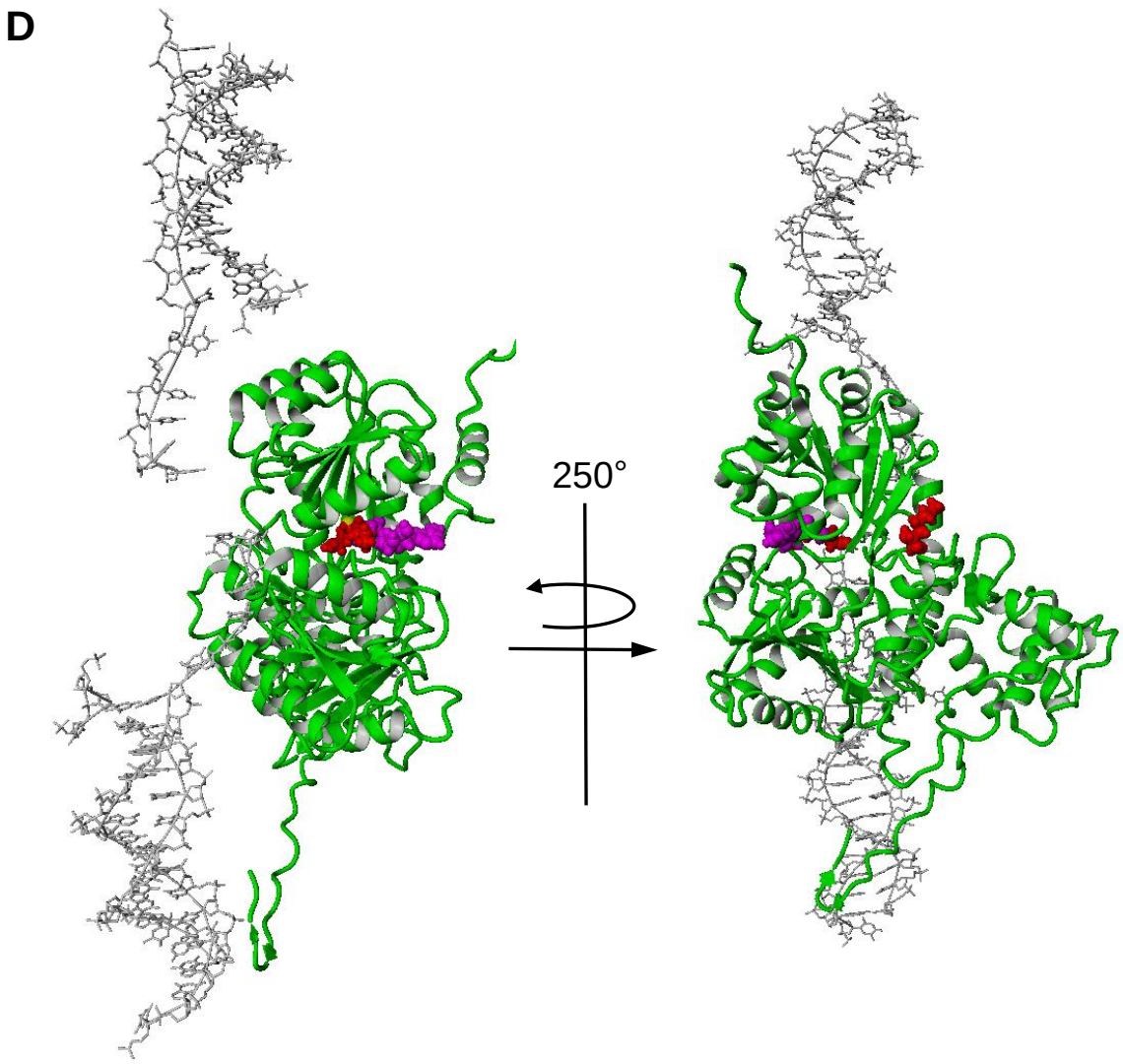

Figure S5

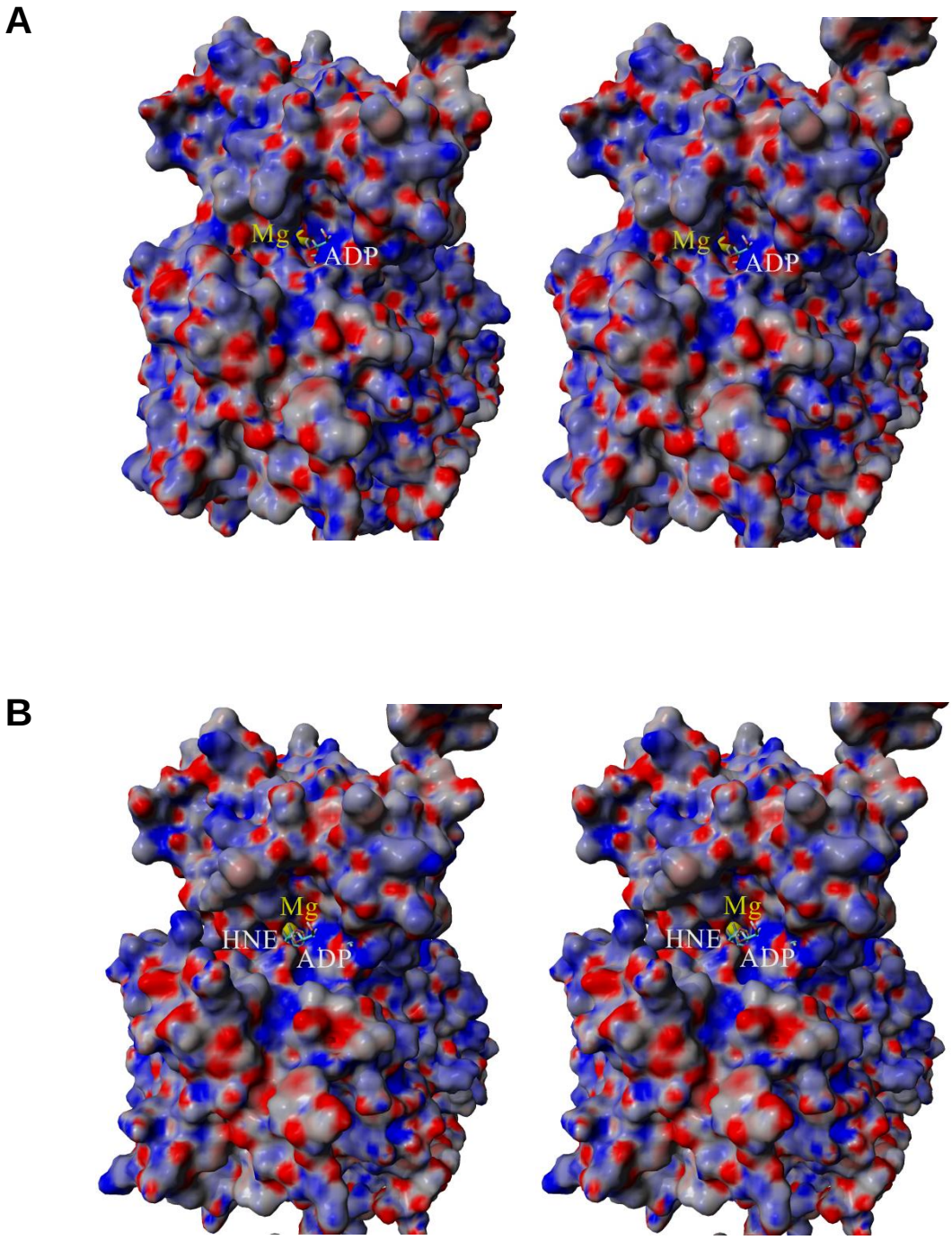

Figure S5

C

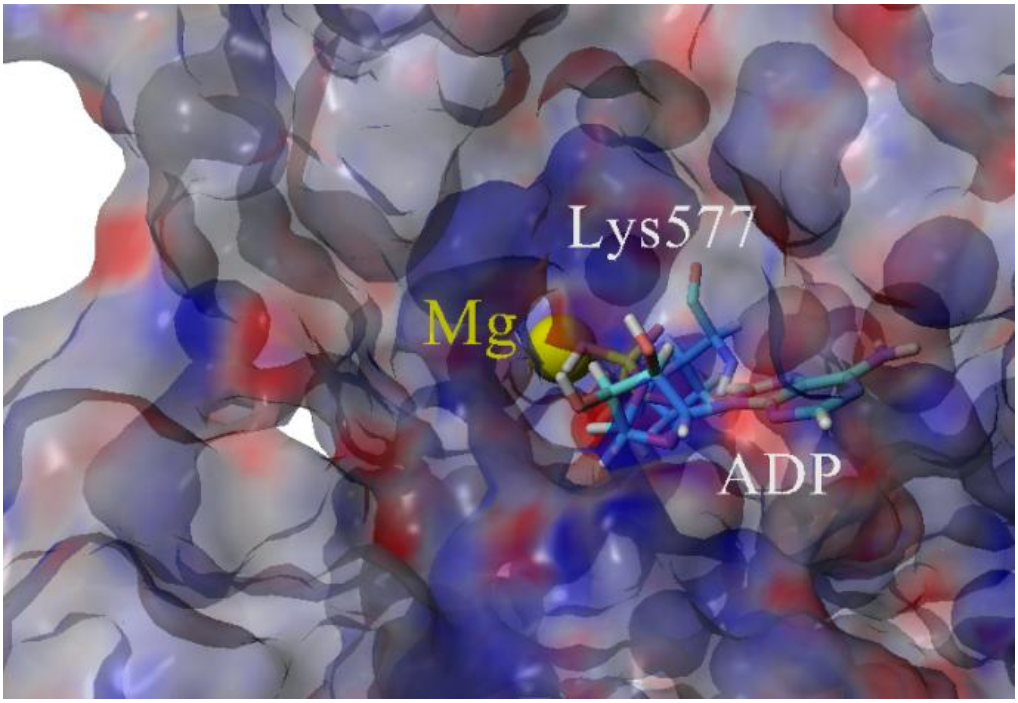

D

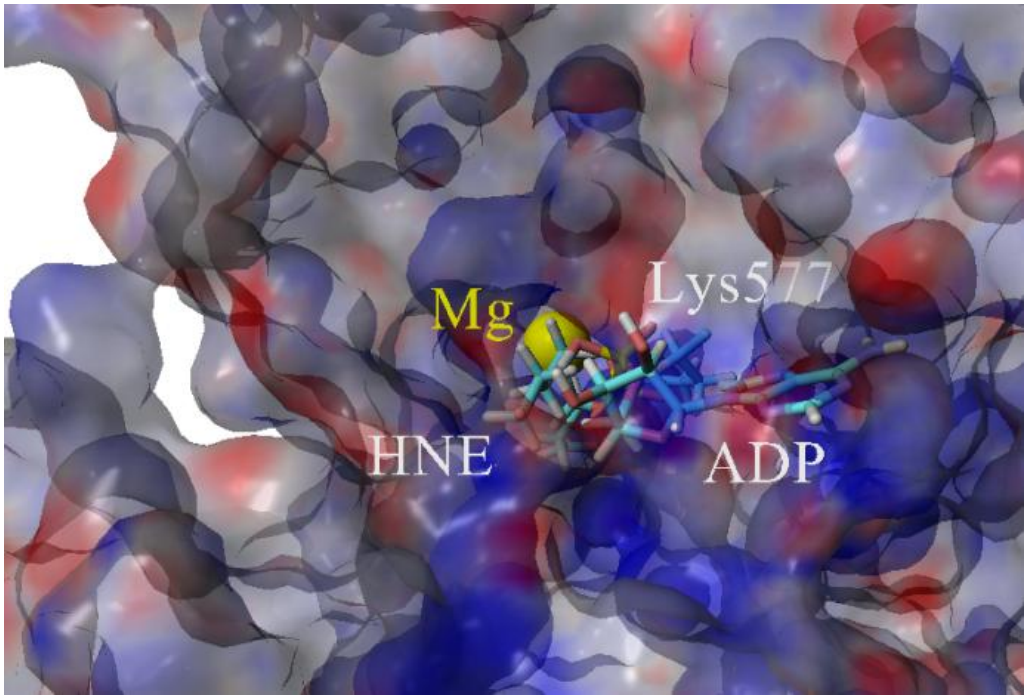

Figure S5

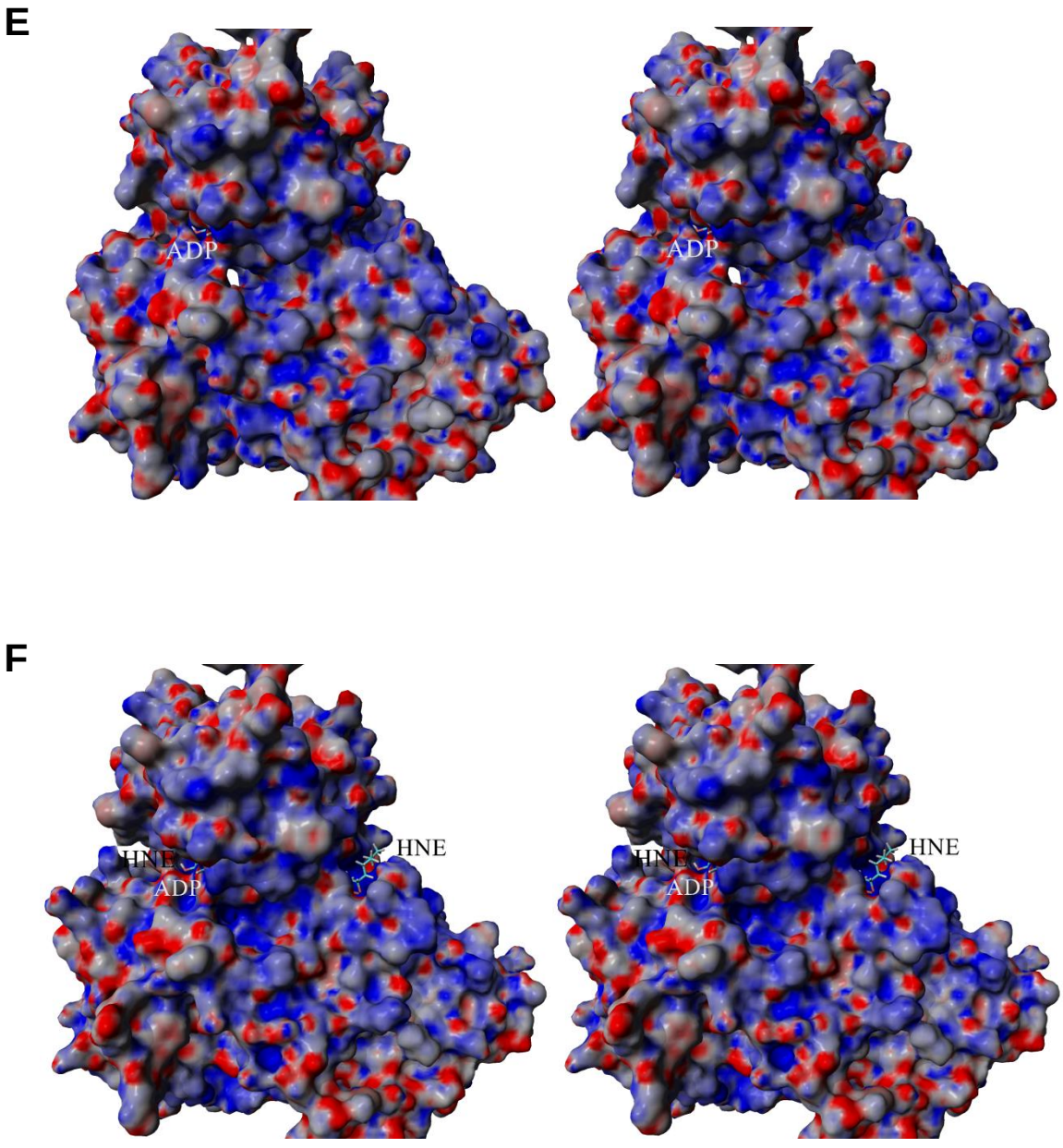

Figure S5

G

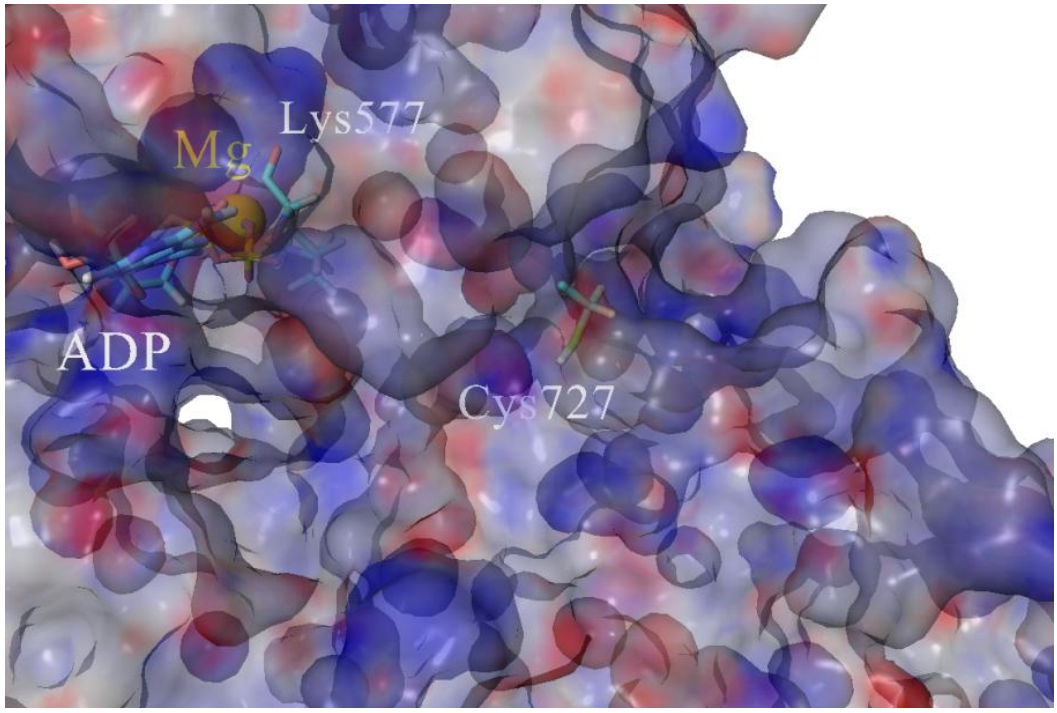
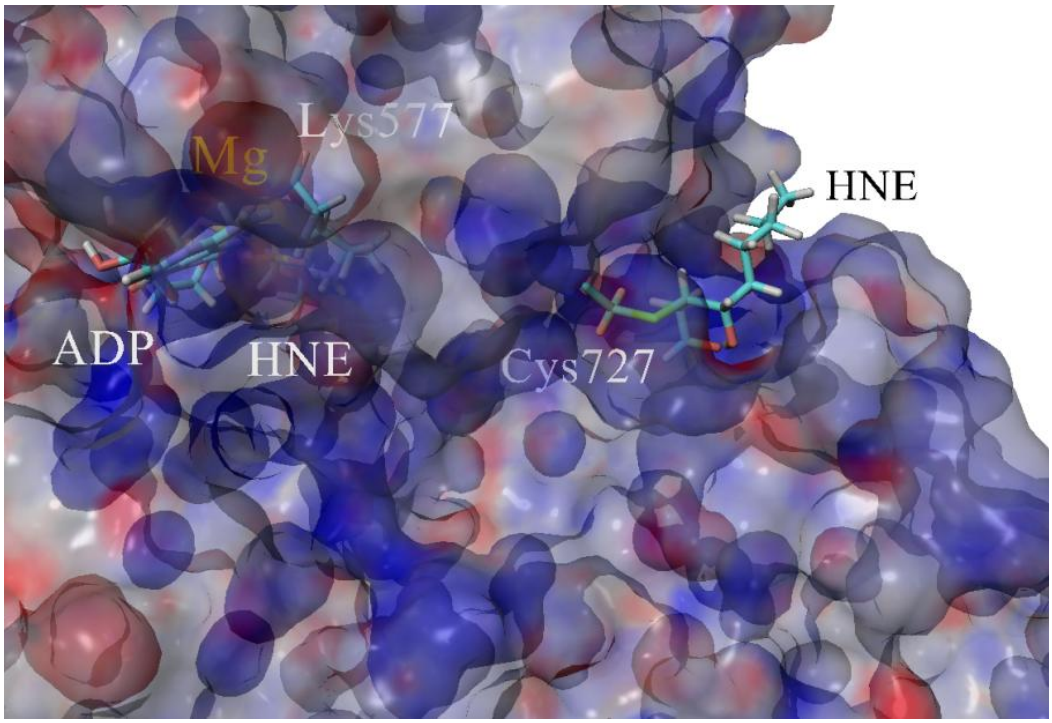
H